Fiber-Reinforced-Cementitious-Composites Plate for Anchoring FRP Sheet on Concrete Member

Qingxu Jin[1] and Christopher K. Y. Leung, M.ASCE[2]

Abstract: To improve the fiber-reinforced polymer (FRP)/concrete bond capacity, this paper presents a new anchoring approach with the gluing of precast fiber-reinforced cementitious composites (FRCC) plate on top of the FRP sheets. In order to measure the improvement in ultimate load and deformation capacity and to study the failure mechanisms around the anchored area, the direct shear bond test is performed on concrete prisms with bonded FRP. Several sets of tests have been carried out with anchoring plates of different FRCC compositions and lengths. Comparison with the control sample shows that the installation of FRCC plate can significantly increase both the bond and deformation capacities (by up to 100%). On the basis of the shear bond test, two types of FRCC plate materials were found to be particularly effective and were selected for strengthening of beam members to be tested under four-point bending. Comparison with control members (without anchor) and those with conventional U-shaped FRP anchors indicates that both the ultimate load and central deflection can be improved by the new anchoring method. **DOI: 10.1061/(ASCE)CC.1943-5614.0000211.** © *2011 American Society of Civil Engineers.*

CE Database subject headings: Fiber-reinforced polymer; Composite materials; Anchors; Bonding; Plates; Shear tests; Sheets; Rehabilitation; Concrete.

Author keywords: Fiber-reinforced polymer; Composite materials; Anchors; Bonding; Plates; Shear tests; Sheets; Retrofitting; Concrete.

Introduction

When fiber-reinforced polymer (FRP) sheets are employed for the flexural or shear strengthening of concrete members, the achievable increase in bond and deformation capacities is often limited by the sudden debonding of the FRP from the concrete substrate. Two major failure modes of FRP debonding are often observed: (1) Concrete cover separation (Ritchie et al. 1991; Garden and Hollaway 1998; Nguyen et al. 2001; Yao and Teng 2007) and (2) Intermediate crack-induced debonding (Ziraba et al. 1994; Rahimi and Hutchinson 2001; Teng et al. 2003; Oehlers et al. 2005; Yao et al. 2005). In order to increase the bond capacity of retrofitted FRP sheets and provide more obvious signs in deformation before failure, the anchoring of FRP sheets has been studied for many years. In previous investigations, various anchoring methods (Fig. 1) have been proposed to enhance the load-carrying capacity of FRP and to delay its debonding.

For example, U-shaped FRP jackets [Fig. 1(a)] applied on the sides and tension face of a beam can be employed to confine the FRP strip and hence to delay the debonding (Teng et al. 2002). In Ceroni (2010), concrete cover separation was observed in a beam member with FRP plate terminated at 300 mm from the support. The test results showed that a U-shaped anchor can enhance the member by 39%. For the beam member with intermediate crack-induced debonding near the midspan rather than high stresses at the plate end, a U-shaped FRP strip anchor shows much less effectiveness. In Smith and Teng (2001), intermediate crack-induced debonding was observed in tested beams with FRP plate terminated at 125 mm from the support. With a U-shaped FRP anchor placed over the end of the FRP, the load capacity only increased slightly from 86.4 kN to 89 kN (a 3% increase). In Leung (2006), FRP-plated beams with a U-shaped anchor at different locations along the FRP were tested under four-point loading. With the anchor at the plate end, there was essentially no increase in load capacity (0.2%). However, the anchoring effect became more significant (13.6%) when the anchor was placed closer to the loading point (750 mm from the plate end).

Fig. 1(b) illustrates the anchoring of FRP with the use of a spike anchor. This method was first proposed by Neuner and Falabella (1996) and further developed by Eshwar et al. (2008). The spike anchor is made up of glass fiber bundles, with part of it impregnated with resin and cured. A hole must be drilled in the concrete member to install the anchor, and resin has to be added afterward. After the first layer (or a couple of layers) of FRP is bonded to the concrete surface, the cured part of the anchor is inserted through the wet FRP layer into the hole, whereas the loose part is spread on top of the FRP later to form a fan. Additional layers of FRP can then be applied. According to the shear bond test results by Eshwar et al. (2008), the effectiveness depends on the embedment depth of the anchor and number of anchors on the strips. As suggested by Özdemir (2005) and Orton et al. (2008), the effective embedment depth for full development of the anchor should be greater than 100 mm to ensure at least a 50 mm depth inside the core of the concrete (beyond the first layer of reinforcing steel). Recently, different configurations of spike anchor have been studied (Niemitz et al. 2010). The results indicate that the failure mode can be converted from FRP debonding to FRP rupture. The percentage increase strongly depends on anchor configuration and varies from 16% to over 40%.

[1]M.Phil., Dept. of Civil and Environmental Engineering, The Hong Kong Univ. of Science and Technology, Clear Water Bay, Hong Kong, China (corresponding author). E-mail: jinqx@ust.hk

[2]Professor, Dept. of Civil and Environmental Engineering, The Hong Kong Univ. of Science and Technology, Clear Water Bay, Hong Kong, China. E-mail: ckleung@ust.hk

Note. This manuscript was submitted on August 31, 2010; approved on February 9, 2011; published online on February 11, 2011. Discussion period open until March 1, 2012; separate discussions must be submitted for individual papers. This paper is part of the ***Journal of Composites for Construction***, Vol. 15, No. 5, October 1, 2011. ©ASCE, ISSN 1090-0268/2011/5-790–798/$25.00.

J. Compos. Constr. 2011.15:790-798.

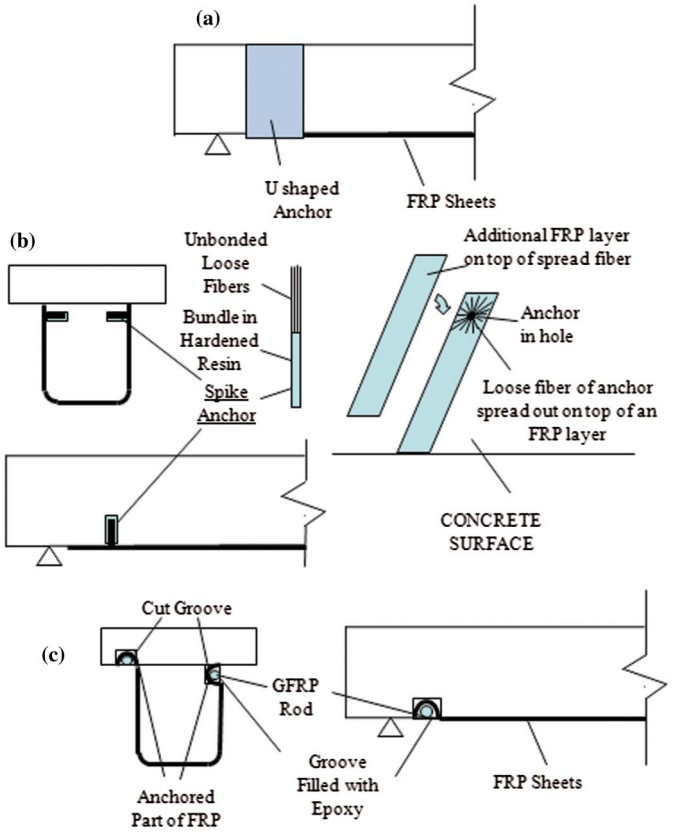

Fig. 1. Various approaches to anchor the FRP strip: (a) U-shaped anchor; (b) spike anchor; (c) NSM FRP anchor

Fig. 1(c) shows the near-surface-mounted (NSM) FRP anchoring technique proposed by Khalifa and Nanni (2000). A groove is cut in the concrete member in which the end of FRP can be inserted. After the groove is half-filled with epoxy, a GFRP rod is inserted before the whole groove is filled. With the plate end embedded, the bond capacity is significantly improved and the failure may occur by FRP rupture instead of debonding (Eshwar et al. 2008). According to results from Eshwar et al. (2008), the larger groove size leads to higher anchorage capacity and the percent increase varies from 7% to more than 30%. The performance of this anchoring technique can also be affected by other construction details; for example, the groove distance from the edge of the member, groove depth, width-to-depth ratio, and the mechanical properties of the groove-filling epoxy (Galati and De Lorenzis 2009).

The existing anchoring methods previously described exhibit a number of limitations. For a U-shaped FRP anchor, the FRP sheets need to be glued to both sides of the member and its bottom surface. For members such as the slab or an edge beam with one side blocked by the wall, it cannot be applied. As shown by Leung (2006), when debonding is induced by an intermediate crack (which is a common situation), it is not effective to put the U-shaped anchor at the plate end. In a four-point bending test, an anchor near the loading point is found to be effective. However, in a real member, loading is not applied through discrete points. It is therefore difficult to determine the location of the anchor for it to be effective. For spike anchors, two limitations can be identified. First, to insert the anchor properly, the hole has to be drilled into the concrete member by more than 100 mm and at least 50 mm inside the core (beyond the concrete cover). In order to prevent the drilled hole from affecting the steel reinforcement, inspection must be carried out in advance to locate the reinforcements. Second, the preparation process for spike anchors is rather complicated. It is time-consuming and requires good workmanship, so the associated cost can be high. Anchoring inside a groove is the most effective among the three methods illustrated in Fig. 1, but it is also the most labor-intensive and expensive. Cutting a groove (especially for a large-sized groove) may affect the existing structural component. In many practical situations, the required strengthening of a beam member is only within 20–30% of the original load capacity. If this can be achieved with simpler techniques, there is no need to go for a complicated retrofitting process such as FRP spike anchorage or thick grooves for FRP anchoring.

The objective of this paper is to propose and study a new and simple anchoring method, which is the gluing of a precast fiber-reinforced cementitious composite (FRCC) plate on top of the FRP sheets. The plate is easy to apply, and no complicated process is involved. The FRCC plate only needs to be applied on the same surface as the retrofitted FRP sheets, so the method is applicable to the flexural strengthening of slabs and edge beams and shear strengthening of beam members. In comparison with spike anchors and grooved anchors, this new anchoring technique is much more economical, as the process is simple and the workmanship requirement is low. Furthermore, this technique only requires surface treatment of the concrete member, so there is no influence on the existing structure. The FRCC plate itself is small and low in weight, so it does not require much material and will only slightly reduce the head room in existing structures.

To verify this method, the strengthened beam member is designed to fail by intermediate crack-induced debonding. When a flexural or shear/flexural crack tends to open at the bottom of the beam, high shear stress will be induced along the FRP/concrete interface to initiate debonding (Leung 2001), which will propagate toward the end of the FRP sheet. The direct shear bond test is employed to simulate the loading condition in the part of the member between a major crack and the support of the beam. It can also be used to measure the debonding resistance of the FRP sheet and its deformation capacity. In the literature, many experimental investigations have been conducted with the asymmetric single shear test (Täljsten 1994, 1997; Yao et al. 2005; Pan and Leung 2007) or the symmetric double shear test (Kobatake et al. 1993; Brosens and Van Gemert 1997; Hiroyuki and Wu 1997). In this paper, the single shear test developed by Pan and Leung (2007) is employed. To study the effects of FRCC composition and plate size on the bond, several sets of specimens are prepared and the details will be described in the next section. The improvement in bond behavior, failure modes and mechanisms for bonding improvement will also be discussed.

On the basis of the results from the direct shear bond test, the most effective FRCC plate anchors are selected for the preparation of strengthened beams to be tested under four-point bending. To assess the applicability of the plate anchor to the concrete beam and compare it with the U-shaped anchor, specimens with different kinds of anchors are prepared and tested. The results will be shown in a subsequent section.

Direct Shear Test

Experimental Program

Material Properties

In the shear bond test, concrete with 50 MPa compressive strength was employed. It has been realized that many old structures need to be strengthened have a lower strength (around 30 MPa). A higher

J. Compos. Constr. 2011.15:790-798.

Table 1. Parameters of the FRCC Plate

Group	FRCC	Cem	FA	SF	Sand[a]	Water	Fiber	L_x[c]	L_y[c]
A/B	NA	A: control; B: width of FRP doubled						NA	NA
C	Plain mortar	1			1.5	0.35		300	100
D	FRCC I	1			1.5	0.35	1%PVA	300	100
E	FRCC II	1			1.5	0.35	0.5%Steel I	300	100
F[b]	PDCC	0.18	0.8	0.02	0.2	0.22	2%PVA	300	100
G[b]	HSFRCC300	1	0.245	0.111	0.865	0.257	2%Steel II	300	100
H[b]	HSFRCC150	1	0.245	0.111	0.865	0.257	2%Steel II	150	100

[a]Groups C, D, and E: river sand, 80 μm to 4.75 mm; group F: single size sand, 53–300 μm; groups G and H: graded silica sand, 53–1,180 μm.
[b]Suitable amounts of SP are added for groups F, G, and H.
[c]L_x and L_y are defined in Fig. 2.

strength is used in our test for the following reasons. First, in developing countries such as China, many recently built structures with strength around 50 MPa are in need of strengthening (as a result of an increase in traffic demand) or repair. Secondly, according to a well-accepted FRP debonding model by Chen and Teng (2001), the bond capacity of FRP on a concrete substrate is proportional to the one-fourth power of the compressive strength ($f_c^{1/4}$). For concrete with strength of 50 MPa and 30 MPa, the difference is only $(50/30)^{1/4}$ or 13.6%. Therefore, it is safe to say that the major conclusions made from the testing of 50 MPa specimens are also valid for 30 MPa specimens. The FRP used in this test was the Reno Composite Material System (Electric Insulator Co., Ltd., Taiwan). According to the properties provided by the manufacturer, the tensile strength for design is 4,200 MPa along the fiber direction and the tensile modulus is 235 GPa. The tensile strength of epoxy resin after complete curing (which takes 7 days) is more than 30 MPa, whereas the shear strength is more than 10 MPa.

To investigate the effects of FRCC composition and plate size on the bond capacity of FRP sheets, eight groups of specimens were prepared for testing. The parameters of FRCC plate are summarized in Table 1. Group A is the control without FRCC plate. Group B was prepared in the same way as group A except that the FRP width is doubled to 100 mm (the same width as concrete prism). To study the contribution of fiber reinforcement, plain mortar plate without fibers was first made by using cement and normal river sand for group C. By using the same mortar composition, different fibers were added to the plates in groups D and E. A 1% volume of PVA fiber was used for group D, whereas 0.5% of steel fiber was employed for group E. These volume fractions are within the typical range for steel and PVA fibers when they are added to mortar or concrete. The properties of fibers are provided in Table 2. For these mixes, the compressive strength was found to be within 40 to 50 MPa. In addition to the normal cementitous matrices, two high-performance cementitous composites were also studied for the FRCC plate anchor. First, pseudoductile cementitious composite (PDCC) was employed in group F. This material exhibits pseudoductile (or strain hardening) tensile behavior as described in Leung and Cao (2009). To achieve such behavior, only fine sand is used in the mix. Second, high-strength fiber-reinforced cementitious composites (HSFRCC) was used to fabricate the plate anchor in group G and group H. The material, with compressive strength over 150 MPa and tensile strength around 9 MPa, was developed in Cheung and Leung (2008). The mechanical properties of different FRCC plate were summarized in Table 3. For groups A–G, the total plate length L was 400 mm (see Fig. 2). The length of FRCC plate on FRP (L_x) was 300 mm whereas the length beyond the plate end (L_y) was 100 mm. For group H, the total plate length L was reduced to 250 mm (with L_x equal to 150 mm). It should be noted that three specimens were prepared and tested for each group.

Table 2. Fiber Properties

Fiber	Diameter (mm)	Length (mm)	E (GPa)	Tensile strength (MPa)	Others
PVA	0.38	12	33	1530	Straight
Steel I	1.08	50	200	1000	Hooked end
Steel II	0.16	13	200	2000	Straight

Specimen Preparation

The specimen for direct shear test consists of a concrete prism with bonded FRP sheets. The anchoring FRCC plate is glued on top of the FRP sheets. In our tests, the size of the concrete prism was 100 mm (width) × 100 mm (depth) × 500 mm (length). Before FRP bonding, the concrete prism was cured for 28 days. The concrete surface was then roughened by using a needle-gun to expose the aggregates. Then a layer of epoxy primer was applied. After the primer hardened for 12 h, four layers of FRP sheets were bonded onto the concrete prism layer by layer with epoxy resin.

Table 3. Properties of FRCC

FRCC type	Compressive strength (MPa)	Tensile strength (MPa)	E (GPa)
FRCC I	35	3	15
FRCC II	50	4–6	20
PDCC	33	3–5	18
HSFRCC	150	9	38

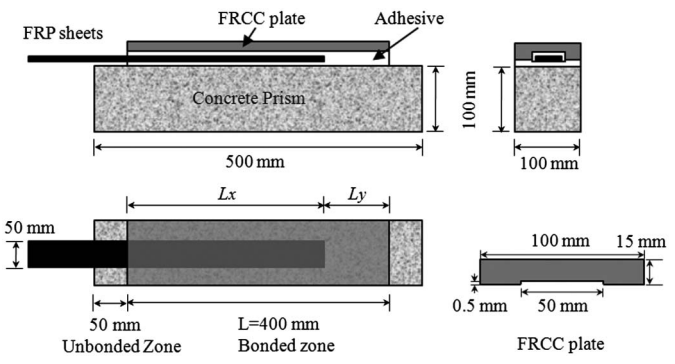

Fig. 2. Test specimen and FRCC plate with detailed dimensions

J. Compos. Constr. 2011.15:790-798.

The bonded FRP sheets were 50 mm (half the width of the concrete prism) in width and 300 mm in length. It should be pointed out that the effectiveness of strengthening depends on the ratio between FRP width and member width (Chen and Teng 2001). When this ratio increases, the effectiveness decreases. It is therefore advantageous to cover part of the width with FRP (to achieve a higher effectiveness) and then further improve the bond capacity by anchoring it at the end. To avoid wedge failure of concrete caused by shear stress in the test, the initial 50 mm of the FRP from the edge of concrete prism was left unbonded (Fig. 2). After the bonding of the FRP sheet, a FRCC plate, extending 100 mm beyond the free end of the sheet, was glued on top of the FRP with another layer of epoxy primer. The FRCC plate was precast, and its size was $100 \times 15 \times 400$ mm. Because the total area of fiber layers was 0.44 mm in thickness (the thickness of the fiber is 0.11 mm per ply), a groove of 0.5 mm in depth and 50 mm in width was introduced in the middle of the bottom side of the plate (Fig. 2). The purpose is to fully cover the FRP sheets while minimizing the gap between the surfaces of FRCC plate and concrete prism where they come into direct contact. To construct the groove, an aluminum plate was first placed in the formwork before the FRCC plate was cast. The aluminum plate was removed during demolding of the FRCC plate. The FRCC plate was cured for 28 days before bonding onto the FRP sheet. The bond test was performed 7 days after sample preparation to ensure full hardening of the epoxy.

Setup and Procedure of Direct Shear Test

Asymmetric direct shear bond test was performed with the testing setup in Fig. 3, developed by Pan and Leung (2007). The concrete specimen was first held tightly in a steel frame to minimize the bending effect on the concrete prism when the FRP sheet was pulled. To apply a pulling force on the FRP sheet, the whole system was installed in the 250 kN material testing system (MTS). The system had to be carefully aligned to ensure that the pulling force would be acting along the vertical plane of the FRP plate so that any peeling effect could be prevented. A linear variable differential transformer (LVDT) was placed beside the specimen to measure the displacement of FRP plate (Fig. 3) relative to the fixed support. The test was conducted under displacement control at the loading rate of 0.1 mm/ min.

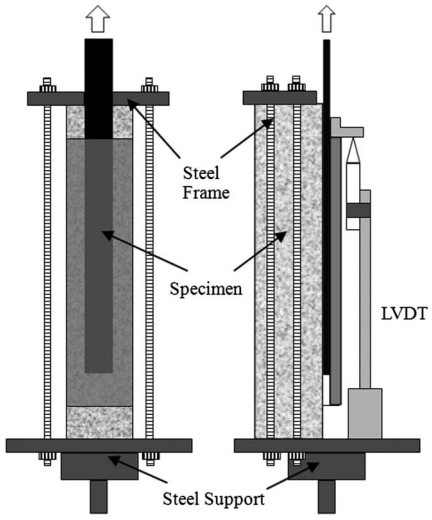

Fig. 3. Test setup for the direct shear test

Test Results and Discussion

All test results are listed in Table 4. For group A, the ultimate load is around 22 kN. The theoretical value is around 18 kN (on the basis of the debonding model in Chen and Teng 2001). The difference between theoretical and test values is quite comparable to those found in Chen and Teng (2001). In comparison with control group A, the percentage improvement of ultimate load capacity and

Table 4. Results of Direct Shear Test

					Impro. (%)	
Grp	Mem	P_u (kN)	D_u (mm)	FM	Load	Displ.
A	1	23.4	1.7	PO	NA	NA
	2	22.3	2.3			
	3	20.8	2.5			
	Aver	22.2	2.2			
	CV	0.059	0.190			
B	1	31.7	2.9	PO	43.7	31.8
	2	32.2	2.2		45	0
	3	32.5	2.5		46.4	13.6
	Aver	32.1	2.5		44.6	13.6
	CV	0.013	0.141		0.033	1.181
C	1	30.1	3.5	MS	35.6	59
	2	33.2	3.8		49.5	72.3
	3	26.7	3		20.3	36.4
	Aver	30	3.4		35.1	54.5
	CV	0.108	0.119		0.416	0.335
D	1	36.8	3.5	I	65.8	59
	2	30.4	2.8	II	36.9	27.3
	3	37	3.3	I	66.7	50
	Aver	34.7	3.2		56.3	45.5
	CV	0.108	0.113		0.301	0.359
E	1	50.1	4.5	I	125.7	104.5
	2	48.2	3.9	I	117.1	77.3
	3	47.9	3.4	I	115.8	54.5
	Aver	49	4		120.7	81.8
	CV	0.025	0.139		0.046	0.309
F	1	33.1	3.8	I	49.1	72.7
	2	35.5	4.1	I	59.9	86.4
	3	28.4	2.8	II	27.9	27.3
	Aver	32.3	3.6		45.5	63.6
	CV	0.112	0.189		0.358	0.487
G	1	41.7	5.3	I	87.8	141
	2	36.1	4	II	62.6	81.8
	3	44.1	4.1	I	98.6	86.4
	Aver	40.6	4.5		82.9	104.5
	CV	0.101	0.161		0.223	0.316
H	1	34.4	5.3	I	54.9	141
	2	36	4	I	62.2	81.8
	3	34.7	3.8	I	55	72.7
	Aver	35	4.4		57.6	100
	CV	0.024	0.185		0.073	0.371

Note: P_u: ultimate load capacity; D_u: ultimate displacement; FM: failure mode. CV: coefficient of variation; PO: peeling off; MS: material shattering; *I*: formation of a major transverse crack in the FRCC plate around the cut-off location of FRP sheet; II: FRCC plate debonded together with the FRP sheet (I and II refer to Fig. 10).

J. Compos. Constr. 2011.15:790-798.

displacement for each specimen can be obtained (Table 4). The average values of ultimate load capacity and displacement and coefficient of variations for each group are also given in Table 4. According to the test results, the bond capacity increased by approximately 50% to more than 100% when the FRCC plate was employed as an anchoring device. Even an unreinforced mortar plate (group C) could enhance the load capacity by 35%. However, failure occurred catastrophically with material shattering in this case, so the use of a plain mortar plate in practice is not recommended and fiber reinforcements should be added. For group B (without FRCC plate), 46% improvement was found in ultimate load capacity by doubling the width of FRP sheets. According to the results in Table 4, a higher load capacity improvement can be obtained by installing a FRCC plate than by simply widening the FRP. For example, the load capacity was improved by 56% and 120% in group D (by adding 1% PVA fibers) and *E* (by adding 0.5% steel fibers), respectively. Because the same mortar was employed in both groups, steel fiber was found to be more effective than PVA fiber in this application. Comparison between the two types of high-performance cementitous composite (43% for PDCC and 83% for HSFRCC) indicates that higher strength is preferable to pseudoductility for the plate anchor. It is of interest to note that the plate made with high-strength fiber composites (HSFRCC) is not as effective as the one with steel fiber–reinforced mortar (FRCCII). The explanation will be provided later in this section.

The ultimate displacement (defined as the displacement at ultimate load) of group B was only 13% higher than that of the control group. We can therefore conclude that doubling the width of FRP sheets was not very effective in increasing the deformation at failure of FRP (and to provide more obvious warning signs). With a bonded FRCC plate, the ultimate displacement was increased more significantly. Even in group C (without fibers), a 45% increase in ultimate displacement was achieved. In groups D and E, the ultimate displacement was increased by 50% and 80%, respectively. The result again shows that steel fiber is preferable to PVA fiber. For high-performance cementitous composites, the ultimate displacement increases by up to 80% with the use of PDCC plate (group F) and is even doubled for HSFRCC plate (groups G and H).

Comparing group G to H, it is interesting to see that the shorter plate (with 150 mm over the FRP) achieves $35/40.6 = 86\%$ of the ultimate load capacity for the longer plate (with 300 mm over the FRP) and the ultimate displacement is almost the same. This high effectiveness indicates that the bonded FRCC plate may play a more significant role around the free end of the FRP. On the basis of the results previously presented, the plates in groups E and G are found to be particularly effective, so they are selected for the preparation of strengthened concrete beams to be tested under four-point bending test. We also observe that group E has higher load-carrying capacity than group G, but its deformation capacity is lower. We believe the surface condition of the anchor plate is playing a significant role. The FRCC plates in group E were prepared with normal sand, whereas the HSFRCC plates in group G only contain very fine particles (see Table 3). As a result, the surface of the HSFRCC plates was much smoother (Fig. 4). It is then easier for interfacial debonding to occur for specimens in group G, and once debonding occurs, the friction is also not as high. The load capacity is therefore lower. With debonding of the anchor plate, it is also easier for the FRP sheet to debond. For a debonded sheet, the average stress (or strain) is much higher than that in a bonded sheet. The measured deformation, which is the total elongation of the FRP, is therefore increased.

In the tests, two modes of failure can be observed. In the first mode (failure mode I), ultimate failure occurred with the formation

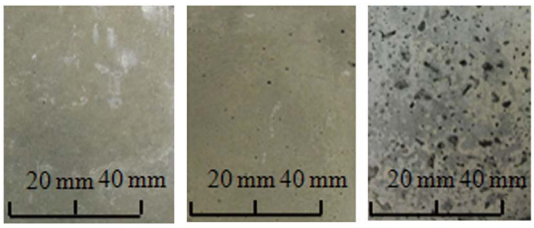

(a) HSFRCC (b) PDCC (c) FRCC II

Fig. 4. Surface of FRCC plate

of a major transverse crack in the FRCC plate around the cut-off location of FRP sheet [Fig. 5(a)]. This failure mode was observed to be most common among our specimens. For this failure mode, multiple cracking does not occur along the plate, so there is no advantage in using a pseudoductile material such as PDCC for the plate. In Fig. 5a, we can also observe that the failure of the debonded part of the FRCC plate, together with FRP sheets, is within the concrete substrate. In the second failure mode (failure mode II), the bonded FRCC plate debonded together with the FRP sheet, and part of debonding is caused by the separation between FRCC plate and resin layer [Fig. 5(b)]. According to the results in Table 2, the second type of failure mode is associated with a reduction of ultimate load and deformation capacity.

Typical load versus displacement curves for groups A, C, E, F, and G are shown in Fig. 5. The improvement in bond capacity with the use of FRCC plate can be explained by various mechanisms. To illustrate the various mechanisms, three forces in equilibrium with the applied loading are shown in Fig. 6. The forces are identified as follows: Force 1 is the shear between FRP sheets and concrete prism; force 2 is the shear between FRCC plate and concrete prism; and force 3 is the tensile force in the FRCC plate at the end of the FRP. In group A and group B, only force 1 is present. As shown in Fig. 5, for the control specimen (group A), when FRP starts to debond, the load drops first and then climbs up again by activating the shear resistance of the remaining area. The debonding would propagate along the concrete substrate until it becomes unstable when ultimate failure occurs. By doubling the width and therefore the bond area of the FRP (as in group B), force 1 is not doubled. As shown in Table 4, the increase is only 46%. This is in agreement with findings in the literature that the load capacity of bonded FRP on a given member is not proportional to its width (Teng et al. 2002; Li et al. 2009). With the FRCC anchoring plate (groups C–H),

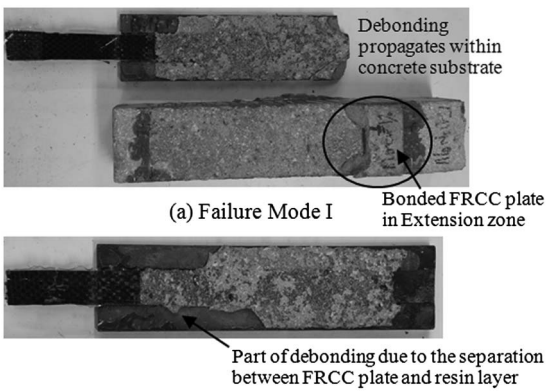

(a) Failure Mode I

(b) Failure Mode II

Fig. 5. Load versus displacement curve for direct shear test

J. Compos. Constr. 2011.15:790-798.

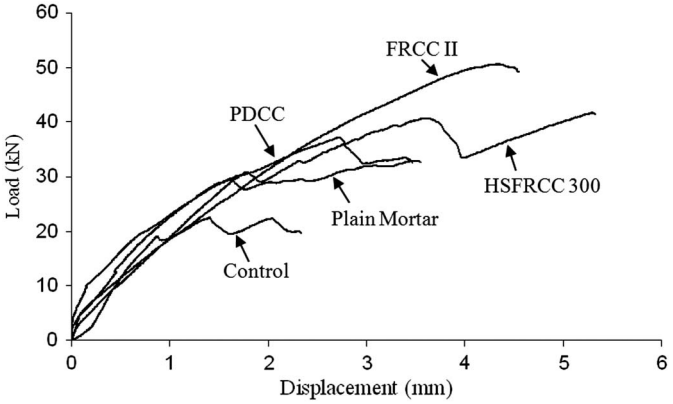

Fig. 6. Force equilibrium; force 1: shear force between FRP sheets and concrete; force 2: shear Force between FRCC plate and concrete; force 3: tensile force at FRCC plate

the total bond area (including FRP/concrete and FRCC/concrete interfaces) is increased relative to the control. Force 2 exists at the FRCC/concrete interface on the two sides of the FRP, whereas force 3 acts on the transverse plane where the FRP terminates. When the applied loading is small, all of it is essentially balanced by force 1 and force 2, so the force at the end of the FRP is negligible. It is obvious that force 2 is dependent on the FRCC/concrete bond. According to Fig. 4, the bonding surface of FRCC II (steel-reinforced mortar) plate is rougher than that for the high-performance cementitious composites (both PDCC and HSFRCC). With larger holes on the FRCC II, the epoxy resin can penetrate into the plate surface more easily. The better bonding ensures debonding within the concrete substrate rather than separation between FRCC plate and resin layer (Failure Modes I and II). As a result, the FRCC II plate provides a higher force 2, which explains the higher ultimate load capacity of group E specimens over the other groups. If FRP debonding occurs before FRCC debonding, force 1 can become higher than that for the unanchored FRP, for the following reason: As observed in the test results, debonding occurs within the concrete and the debonded region exhibits an undulating surface. When the debonded FRP is pulled, interfacial sliding is coupled with displacements perpendicular to the interface. With the FRP covered by a FRCC plate bonded to the concrete (on the two sides of the FRP and also beyond its end), the normal displacement is resisted and normal compression is induced to increase the friction along the debonded interface. Force 1 therefore increases. With increasing loading, debonding will occur along both the FRP/concrete and FRCC/concrete interfaces. Force 1 and force 2 will then decrease while force 3 increases to maintain equilibrium. With the presence of force 3, unstable debonding is delayed so the deformation at failure is significantly improved. Plates with smoother surface (such as HSFRCC plate) can elongate more as there is little friction along the plate/concrete interface. As a result, they exhibit higher deformation at failure (Fig. 5). However, with the smoother surface, Type II failure is also more likely to occur.

Simple calculations can be performed to estimate the contributions of each force component to the bond capacity. Because groups E and G showed the best performance among the eight groups, these two cases are picked as examples. According to the results in Table 4, the total force (or load capacity) is $P_E = 49$ kN and $P_G = 40$ kN for groups E and G, respectively. The tensile strength of FRCC II is taken to be 5 MPa (10% of compressive strength), whereas that for the HSFRCC was measured to be 9 MPa. With the cross-section area of plate being $1,500$ mm^2, the maximum possible value of force 3 for group E and group G equals 7.5 kN (FRCC II) and 13.5 kN (HSFRCC), respectively. In reality, this value may not be reached, as debonding can occur along the plate beyond the end of the FRP. However, by using this overestimated value of force 3, an underestimated value of force 1 plus force 2 is calculated to be 41.5 kN (49-7.5) for group E and 26.5 kN (40-13.5) for group G. Comparing the overestimated value of force 3 to the underestimated value of force 1 plus force 2, it is clear that force 1 plus force 2 contributes more to the bond capacity than force 3.

In the preceding paragraphs, we have made a conjecture that the anchoring plate can impose normal compressive force on the FRP to increase force 1. As it is hard to separate force 1 from force 2, force 1 plus force 2 for group E is compared with the bond capacity of group B to see if the presence of the plate has indeed increased the interfacial resistance. The area covered by the full-width FRP in group B specimens is exactly the same as the area under force 1 plus force 2 in group E specimens. In group B, the ultimate bond capacity is 32.1 kN, which is lower than the underestimated value of force 1 plus force 2 (equals 41.5 kN) in group E. The difference in interfacial resistance under the same area can be explained by the increased friction caused by normal compressive force.

For each group of specimens, the coefficient of variation is also provided in Table 4. According to the calculated values, the variation within groups with the same failure mode is lower than that for groups with different failure modes. Moreover, it is interesting to notice that the ultimate displacement shows higher variation than the ultimate load capacity.

Four-Point Bending Test

Experimental Program

Specimen Preparation and Material Properties

In order to demonstrate the new anchoring method, a 2-m-long concrete beam with retrofitted carbon FRP sheets was prepared for the four-point bending test. The cross section is 200 mm in depth and 150 mm in width. The design details of the steel reinforcement are shown in Fig. 7, and the reinforcement ratio was the same (around 1%) in all the tested beams. The beams were all underreinforced with high-yield steel bars: two 10 mm tension bars, two 10 mm compression bars, and 8 mm steel stirrups at 75 mm spacing. The cover to stirrups was nominal (30 mm). The RC beam alone was designed for flexural failure well before failure in shear. We avoided the failure of concrete crushing by adding two compressive steel bars. The grade of concrete was 50 MPa (the same as direct shear test specimens). The concrete beam and FRCC plate were first cured for 28 days. After roughening the tension side of the beam, carbon FRP sheets were bonded. After bonding the FRP sheets, different anchors were applied at the end. The distance between the support and anchor was 50 mm.

To investigate the effectiveness of this new anchoring method, four groups of specimens were prepared with four layers of bonded FRP sheets (FRP reinforcement ratio is 0.11%). Group B1 (concrete beam with retrofitted carbon FRP sheets) was the control

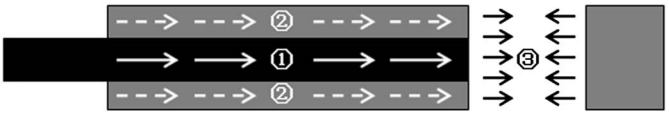

Fig. 7. Load versus displacement curve for four-point bending test

J. Compos. Constr. 2011.15:790-798.

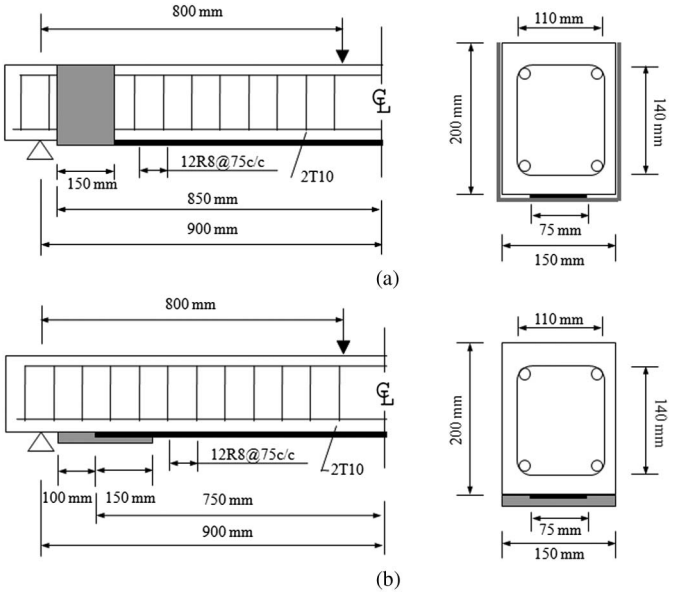

Fig. 8. Design details for (a) group B; (b) group BU

without end anchorage. The length of bonded FRP sheets was 1700 mm and the width of FRP sheets was 75 mm (half of the beam width). To compare the FRCC plate anchor with the conventional anchoring method, U-shaped carbon FRP anchors (150 mm in width) were applied to specimens in group BU [Fig. 8(a)]. In this case, the length of FRP sheets was kept at 1,700 mm. To study the effect of the plate anchor, two types of FRCC plate, prepared with FRCC II and HSFRCC, were employed in group BP-F and group BP-H, respectively. The configuration of the specimens in these two groups is illustrated in Fig. 8(b). When the plate anchor was used, the FRP length was reduced to 1,500 mm with the plate extending 100 mm from each side of the FRP so the distance between support and the edge of FRCC anchor is 50 mm. In both cases, the size of the FRCC plate was 150 mm (width) × 20 mm (depth) × 250 mm (length), with a middle groove 0.5 mm in depth and 75 mm in width. The parameters for each group are summarized in Table 5. For each group, two specimens were prepared and tested.

Setup and Procedure of the Four-Point Bending Test

The test was performed 7 days after sample preparation to ensure full hardening of the epoxy. All the beam members were subjected to four-point loading, with equal forces applied at a distance of 800 mm from the two supports (Fig. 8). Beam member was set up on the 500 kN material testing system (MTS) with a loading span L of 1,800 mm. A linear variable differential transformer (LVDT) was placed at the bottom of the beam to measure the middle deflection. The test was conducted under displacement control at the loading rate of 0.5 mm/ min.

Test Results and Discussion

For all specimens, intermediate crack-induced debonding was found to initiate from the flexural crack in the shear span that is closest to the loading point. (Note: in postfailure inspection, the debonding zone was found to extend from the end of the FRP to such a crack.) All the test results are summarized in Table 5, and a typical load versus deflection curve is provided in Fig. 7. According to Fig. 7, the load stays at a flat plateau after a sudden drop from the peak load. The result indicates that the tension steel has already yielded when the specimen reaches its peak load. Because the retrofitted FRP does not carry any loading after debonding, the residual load capacity should equal the ultimate load capacity of the unstrengthened beam member. This argument is supported by the testing results from Lee et al. (2004), which are shown in Fig. 9. For the beams tested in this investigation, the average postpeak load (at the plateau) for all specimens was found to be 45.3 kN. The load contributed by the FRP or FRP plus anchor is obtained by subtracting this residual load from the peak load in each test. The results are provided in the sixth column of Table 5. From the shape of the load displacement curve, the steel reinforcements should have yielded before FRP debonding occurs. At the ultimate load, with the plane section remaining plane assumption, the neutral axis location can be obtained from force equilibrium and the FRP force can be calculated by moment equilibrium (Li et al. 2009). The results are given in the seventh column of Table 5. The improvement by adding anchorage is equal to the difference of the load carried by FRP sheets between groups with anchor (groups BU, BP-F, and BP-H) and the control group with no anchor (group B1). The percentage improvement in bond capacity by the plate anchor (I_f) is calculated from

$$I_f = [N_{(\text{anchor})} - N_{(B1)}]/N_{(B1)}$$

Table 5. Parameters and Results of Four-Point Bending Test

Group	Anchor method	Anchor material	MemNo.	P_m (kN)	P_c (kN)	N (kN)	I_f (%)	D (mm)	I_d (%)	Failure mode
B1	NA	NA	1	69.3	24	96	NA	16.2	NA	FD
			2	66.9	21.6	86.4	NA	15.4	NA	FD
			Ave	68.1	22.8	91.2	NA	15.8	NA	
BU	U-shaped	CFRP	1	69.1	23.8	95.2	4.4	19.3	22	FR
			2	68.4	23.1	84	1.3	18.4	16.5	FR
			Ave	68.8	23.5	94	3	18.9	19.6	
BP-F	Plate	FRCC II	1	74.8	29.5	118	29.4	22.1	39.9	I
			2	73.4	28.1	112.4	23.3	20.8	31.6	I
			Ave	74.1	28.8	115.2	26.3	21.4	35.4	
BP-H	Plate	HSFRCC	1	69.8	24.5	98	7.5	23.6	49.4	I
			2	66.8	21.5	86	−5.7	17.6	11.4	II
			Ave	68.3	23	92	0.9	20.6	30.3	

Note: P_m: maximum applied load (kN); P_c: contribution by FRP or FRP plus anchor (kN); N: force carried by FRP sheets; I_f: improvement of bond capacity by anchor (%); D: ultimate central deflection (mm); I_d: improvement of deformation capacity by anchor (%). FD: FRP debonding; FR: rupture of U-shaped FRP anchor; I and II: failure mode in direct shear test.

J. Compos. Constr. 2011.15:790-798.

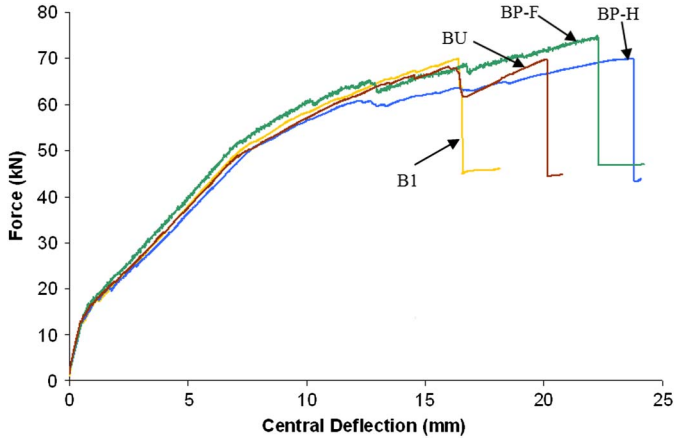

Fig. 9. Comparison of residual load after FRP debonding in the strengthened beam with unstrengthened beam (Lee et al. 2004, reprinted with permission from The Hong Kong University of Science and Technology)

in which $N_{(anchor)}$ = force carried by FRP sheets with anchor, BU, BP-F, or BP-H and $N_{(B1)}$ = load carried by FRP without anchor (Control).

For the load capacity improvement, the U-shaped anchor only contributes 3%, although the FRCC II plate anchor is able to provide 26.3%. For the BP-H specimens, if failure mode I is observed, the load capacity can be increased by 7%. If failure mode II occurred, the value is similar to control specimens without anchor, so the effect of the anchor is minimal. The results show that FRCC plates with a smooth surface are not as effective as those with a rougher surface.

The central deflection improvement represents the increasing signs of warning against FRP debonding. The percentage is calculated in the same way as load capacity improvement. The member with the U-shaped anchor shows a 19.6% increase over the control whereas FRCC plate gives much higher improvement (35.4% for FRCC II plate and 30.3% for HSFRCC plate). In general, similar values of ultimate load and central deflection were observed in both specimens in each group. However, relatively lower values (ultimate load of 66.8 kN and central deflection of 17.6 mm) were observed in one of the specimens in BP-H. This is because failure in this case occurred by the debonding of anchoring plate with the FRP (Mode II in Fig. 10) rather than plate cracking at the FRP end (Mode I in Fig. 10). For group BP-F, plate cracking at the FRP end (Mode I) was observed in both specimens. The finding is consistent with those from the direct shear test, which indicates (1) Mode II failure is possible for the HSFRCC plate (see Table 4), and (II) the load capacity for Mode II failure is lower than that for Mode I.

The member with the FRCC II plate anchor exhibits higher load-carrying capacity in both the shear bond test and the beam test. Quantitatively, however, the anchor is found to be far more effective in improving the performance in the shear bond test than that in the beam. The explanation is as follows. In the shear bond test, the load is directly applied on a very short length of FRP and the anchorage is activated almost immediately when the FRP is pulled. In the four-point bending test, the debonding failure is initiated by a crack in the middle of the concrete beam. For an unanchored FRP, the debonded zone propagates under a constant load P until it becomes unstable [Fig. 11(a)]. For the anchored FRP, the debonded zone has to reach the anchor before the anchor resistance, P_{anchor}, can be activated [Fig. 11(b)]. If the anchor is placed far away from the middle of the beam, the contribution of anchor to the total bond force is compromised by the decreased load-carrying capacity along the debonded interface as a result of shear softening [see Fig. 11(b)]. In other words, when the anchor force is increased to its peak value, the shear stresses along the unanchored part of the FRP may have significantly decreased. Because it is not possible to add the contribution of the anchored part directly to the load capacity of the unanchored FRP, the percentage improvement is much lower than that in the shear bond test. However, on the basis of the test results, if the right material

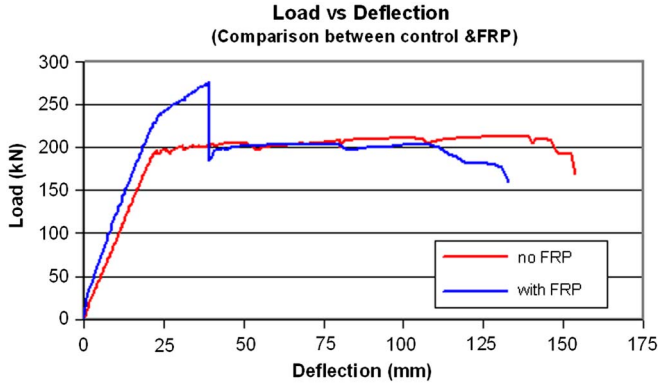

Fig. 10. Failure modes of specimens

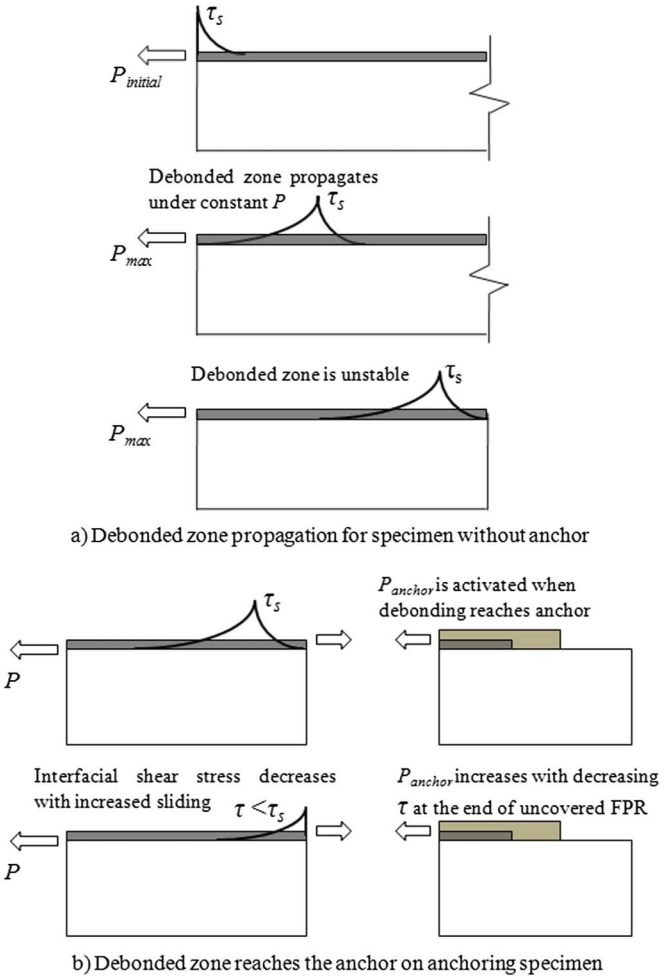

Fig. 11. Debonded zone propagation and shear softening

J. Compos. Constr. 2011.15:790-798.

(FRCC II in this case) is chosen for making the plate, significant improvement of load capacity can still be achieved (Table 5).

Conclusion

In this paper, a direct shear test was conducted to study whether the debonding load capacity of FRP sheets on a concrete member can be enhanced by the use of a glued FRCC plate as an anchor. We investigated the effects of FRCC composition and plate length. With the FRCC plate, both the debonding load capacity and deformation capacity are found to increase considerably. We discuss the plausible mechanisms for performance improvement. On the basis of the test results, the effectiveness of FRCC plate appears to have a correlation with the surface roughness of the FRCC plate. Based on the shear bond test, two types of FRCC plate materials were found to be particularly effective and selected for strengthening of beam members that are tested under four-point bending. The beam test results indicate that a plate anchor made with the appropriate FRCC material performs much better than the conventional U-shaped FRP anchor. Comparing the control beam with unanchored FRP, both the load capacity and deformation at failure are improved, by 26% and 36%, respectively. In the present study, we demonstrate the applicability of the plate anchor as a simple and effective method to resist debonding of FRP.

References

Brosens, K., and van Gemert, D. (1997). "Anchoring stresses between concrete and carbon fiber reinforced laminates." *Non-metallic (FRP) Reinforcement for Concrete Structures, Proc., 3rd Int. Symp.*, Sapporo, Japan, 271–278.

Ceroni, F. (2010). "Experimental performances of RC beams strengthened with FRP materials." *Constr. Build. Mater.*, 24(9), 1547–1559.

Chen, J. F., and Teng, J. G. (2001). "Anchorage strength mode for FRP and steel plates bonded to concrete." *J. Struct. Eng.*, 127(1), 784–791.

Cheung, A. K. F., and Leung, C. K. Y. (2008). "Experimental study on the bond between steel reinforcement and self-compacting high strength fiber reinforced cementitious composites." *Proc., 7th Int. RILEM Symp. on Fibre Reinforced Concrete: Design and applications BEFIB*, RILEM, Chennai, India, 667–678.

Eshwar, N., Nanni, A., and Ibell, T. J. (2008). "Performance of two anchor systems of externally bonded fiber-reinforced polymer laminates." *ACI Mater. J.*, 105(1), 72–80.

Galati, D., and De Lorenzis, L. (2009). "Effect of construction details on the bond performance of NSM FRP bars in concrete." *Adv. Struct. Eng.*, 12(5), 683–700.

Garden, H. N., and Hollaway, L. C. (1998). "An experimental study of the influence of plate end anchorage of carbon fiber composite plates used to strengthen reinforced concrete beams." *Compos. Struct.*, 42(2), 175–188.

Hiroyuki, Y., and Wu, Z. (1997). "Analysis of debonding fracture properties of CFS strengthened member subject to tension." *Non-Metallic (FRP) Reinforcement for Concrete Structures, Proc., 3rd Int. Symp.*, Japan Concrete Inst., Sapporo, Japan, 287–294.

Khalifa, A., and Nanni, A. (2000). "Improving shear capacity of existing RC *T*-section beams using CFRP composites." *Cem. Concr. Compos.*, 22, 165–174.

Kobataka, Y., Kimura, K., and Katsumata, H. (1993). "A retrofitting method for reinforced concrete structures using carbon fiber." *Fiber reinforced plastic reinforcement for concrete structures: Properties and applications*, A. Nanni, ed., Elsevier, Amsterdam, 435–450.

Lee, S., Leung, C. K. Y., Chen, Z., Xu, M., and Tang, J. M. (2004). "Design guidelines for strengthening concrete structures using externally bonded fiber reinforced plastic systems." *HKUST Advanced Engineering Materials Facility Research Rep.*

Leung, C. K. Y. (2001). "Delamination failure in concrete beams retrofitted with a bonded plate." *J. Mater. Civ. Eng.*, 13, 106–113.

Leung, C. K. Y. (2006). "FRP debonding from a concrete substrate: Some recent findings against conventional belief." *Cem. Concr. Compos.*, 28, 742–748.

Leung, C. K. Y., and Cao, Q. (2009). "Development of strain hardening permanent formwork for durable concrete structures." *Mater. Struct.*, 43(7), 993–1007.

Li, Z, Leung, C. K. Y., and Xi, Y. (2009). *Structural renovation in concrete*, Taylor and Francis, Oxon, U.K.

Neuner, J., and Falabella, R. (1996). "Composite anchor system: Flatwise tensile and shear testing." *Internal Rep.*, Hexcel, Stamford, CT.

Nguyen, D. M., Chan, T. K., and Cheong, H. K. (2001). "Brittle failure and bond development length of CFRP-concrete beams." *J. Compos. Constr.*, 5(1), 12–17.

Niemitz, C. W., James, R., and Berña, S. F. (2010). "Experimental behavior of carbon fiber-reinforced polymer (CFRP) sheets attached to concrete surfaces using CFRP anchors." *J. Compos. Constr.*, 12(2), 185–194.

Oehlers, D. J., Liu, I. S. T., and Seracino, R. (2005). "Shear deformation debonding of adhesively bonded plates." *Proc. Inst. Civ. Eng.*, 158(1), 77–84.

Orton, S. L., Jirsa, J. O., and Beyrak, O. (2008). "Design considerations of carbon fiber anchors." *J. Compos. Constr.*, 12(6), 608–616.

Özdemir, G. (2005). "Mechanical properties of CFRP anchorages." Master of Science thesis, Middle East Tech. Univ., Istanbul, Turkey.

Pan, J. L., and Leung, C. K. Y. (2007). "Effect of concrete composition on FRP/concrete bond capacity." *J. Compos. Constr.*, 11(6), 611–618.

Rahimi, H., and Hutchinson, A. (2001). "Concrete beams strengthened with externally bonded FRP plates." *J. Compos. Constr.*, 5(1), 44–56.

Ritchie, P. A., Thomas, D. A., Lu, L. W., and Connelly, G. M. (1991). "External reinforcement of concrete beams using fiber reinforced plastic." *ACI Struct. J.*, 88(4), 490–500.

Smith, S. T., and Teng, J. G. (2001). "Debonding failures in FRP-plated RC Beams with or without U strip end anchorage." *Proc., FRP Composites in Civil Engineering*, 1, 607–615.

Täljsten, B. (1994). "Plate bonding. Strengthening of existing concrete structures with epoxy bonded plates of steel or fibre reinforced plastics." Ph.D. thesis, University of Technology, Luleá, Sweden.

Täljsten, B. (1997). "Strengthening of beams by plate bonding." *J. Mater. Civ. Eng.*, 9(4), 206–212.

Teng, J. G., Chen, J. F., Smith, S. T., and Lam, L. (2002). *FRP strengthened RC structures*, Wiley, West Sussex, U.K.

Teng, J. G., Smith, S. T., Yao, J., and Chen, J. F. (2003). "Intermediate crack-induced debonding in RC beams and slabs." *Constr. Build. Mater.*, 17(6–7), 447–462.

Yao, J., and Teng, J. G. (2007). "Plate end debonding in FRP-plated RC beams—I: Experiments." *Eng. Struct.*, 29(10), 2457–2471.

Yao, J., Teng, J. G., and Lam, L. (2005). "Experimental study on intermediate crack debonding in FRP-strengthened RC flexural members." *Adv. Struct. Eng.*, 8(4), 365–396.

Ziraba, Y. N., Baluch, M. H., Basunbul, I. A., Sharif, A. M., Azad, A. K., and Al-Sulaimani, G. J. (1994). "Guideline towards the design of reinforced concrete beams with external plates." *ACI Struct. J.*, 91(6), 639–646.

J. Compos. Constr. 2011.15:790-798.